An ab Initio Investigation of the Structure and Alkali Metal Cation Selectivity of 18-Crown-6

Eric D. Glendening,* David Feller, and Mark A. Thompson

Contribution from the Molecular Science Research Center, Pacific Northwest Laboratory, Richland, Washington 99352

Received April 13, 1994[⊗]

Abstract: We present an ab initio, quantum mechanical study of 18-crown-6 (18c6) and its interaction with the alkali metal cations Li^+, Na^+, K^+, Rb^+, and Cs^+. Geometries, binding energies, and binding enthalpies are evaluated at the restricted Hartree−Fock (RHF) level using standard basis sets (3-21G and 6-31+G*) and relativistic effective core potentials. Electron correlation effects are determined at the MP2 level, and wave function analysis is performed by the natural bond orbital (NBO) and associated methods. The affinity of 18c6 for the alkali metal cations is quite strong (50−100 kcal mol^{-1}, depending on cation type), arising largely from the electrostatic (ionic) interaction of the cation with the nucleophilic ether backbone. Charge transfer (covalent bonding) contributions are somewhat less important, only 20−50% as strong as the electrostatic interaction. Agreement of the calculated binding enthalpies and experimentally determined quantities is rather poor. For example, the binding energy for K^+/18c6 (−71.5 kcal mol^{-1}) is about 30 kcal mol^{-1} stronger than that determined by experiment, and it is not clear how to reconcile this difference. Our calculations clearly show that solvation effects strongly influence cation selectivity. Gas-phase 18c6 preferentially binds Li^+, not K^+ as found in aqueous environments. We show, however, that K^+ selectivity is recovered when even a few waters of hydration are considered.

I. Introduction

Macrocyclic polyethers (or crown ethers) have received widespread attention since they were first characterized by Pedersen in the late 1960s.[1,2] Much of this interest stems from their ability to selectively bind various cations in solution, depending in part on the size of the crown ether, the type of donor atom (e.g., oxygen, nitrogen, sulfur), and solvent polarity. There is presently available a wealth of thermodynamic[3,4] and structural data[5] for a host of crown ethers. Computational chemists are also increasingly interested in crown ethers as they perhaps represent the simplest molecules that exhibit enzyme-like specificity in their interactions with cations. In particular, 18-crown-6 (18c6) has been the focus of a number of molecular mechanics,[6,7] molecular dynamics,[8−13] and Monte Carlo investigations.[14,15] These have provided a rather detailed description of the important conformations sampled in both gas- and condensed-phases and of the crown ether interactions with cations and solvent molecules.

The number of investigations of the electronic structure of 18c6 is, however, rather limited. Yamabe *et al.*[16] reported a CNDO/2 study of gas-phase crown ether and its interaction with Na^+ and K^+. Their calculations suggested that charge transfer is largely responsible for the cation/crown ether interaction and that selectivity of 18c6 is strongly influenced by competition between the crown ether and solvent molecules for the cation. These views were subsequently corroborated by the same authors using minimal basis set ab initio methods.[17] More recently, Ha and Chakraborty[18] examined the interaction of 18c6 with ammonium cation. Partial geometry optimizations of the crown ether and its cation complex were performed with a density functional theory approach to generate a potential energy function for subsequent Monte Carlo simulations.[15] In the present work, we report extended basis set ab initio calculations of the structure, binding affinities, and cation selectivity of 18c6. To the best of our knowledge, this work presents the highest level calculations to date of the electronic structure of a crown ether and its cation complexes. The only other polarized basis set investigation of which we are aware is the work of Seidl and Schaefer[19] on low-lying conformations of 12-crown-4.

Our interest in crown ethers stems primarily from their potential application as sequestering agents for radionuclides in the treatment of nuclear waste streams and contaminated soils. Horwitz, Dietz, and Fisher[20] reported a process (SREX) involving di-*tert*-butylcyclohexano-18-crown-6 for recovering strontium-90 from acidic solution. This process is particularly important

⊗ Abstract published in *Advance ACS Abstracts,* October 1, 1994.

(1) (a) Pedersen, C. J. *J. Am. Chem. Soc.* **1967**, *89*, 2495. Also, see: (b) Pedersen, C. J. *Angew. Chem., Int. Ed. Engl.* **1988**, *27*, 1021, and references therein.

(2) (a) Cram, D. J. *Angew. Chem., Int. Ed. Engl.* **1988**, *27*, 1009. (b) Lehn, J.-M. *Angew. Chem., Int. Ed. Engl.* **1988**, *27*, 89 and references therein.

(3) De Jong, F.; Reinhoudt, D. N. *Adv. Phys. Org. Chem.* **1980**, *17*, 279, and references therein.

(4) Izatt, R. M.; Bradshaw, J. S.; Nielsen, S. A.; Lamb, J. D.; Sen, D.; Christensen, J. J. *Chem. Rev.* **1985**, *85*, 271.

(5) Dale, J. *Isr. J. Chem.* **1980**, *20*, 3.

(6) Wipff, G.; Weiner, P.; Kollman, P. *J. Am. Chem. Soc.* **1982**, *104*, 3249.

(7) Hancock, R. D. *Acc. Chem. Res.* **1990**, *23*, 253 and references therein.

(8) Howard, A. E.; Singh, U. C.; Billeter, M.; Kollman, P. A. *J. Am. Chem. Soc.* **1988**, *110*, 6984.

(9) van Eerden, J.; Harkema, S.; Feil, D. *J. Phys. Chem.* **1988**, *92*, 5076.

(10) Straatsma, T. P.; McCammon, J. A. *J. Chem. Phys.* **1989**, *91*, 3631.

(11) Dang, L. X.; Kollman, P. *J. Am. Chem. Soc.* **1990**, *112*, 5716.

(12) Sun, Y.; Kollman, P. A. *J. Chem. Phys.* **1992**, *97*, 5108.

(13) Leuwerink, F. T. H.; Harkema, S.; Briels, W. J.; Feil, D. *J. Comput. Chem.* **1993**, *14*, 899.

(14) Ha, Y. L.; Chakraborty, A. K. *J. Phys. Chem.* **1991**, *95*, 10781.

(15) Ha, Y. L.; Chakraborty, A. K. *J. Phys. Chem.* **1993**, *97*, 11291.

(16) Yamabe, T.; Hori, K.; Akagi, K.; Fukui, K. *Tetrahedron* **1979**, *35*, 1065.

(17) Hori, K.; Yamada, H.; Yamabe, T. *Tetrahedron* **1983**, *39*, 67.

(18) Ha, Y. L.; Chakraborty, A. K. *J. Phys. Chem.* **1992**, *96*, 6410.

(19) Seidl, E. T.; Schaefer, H. F., III *J. Phys. Chem.* **1991**, *95*, 3589.

(20) (a) Horwitz, E. P.; Dietz, M. L.; Fisher, D. E. *Solvent Extraction and Ion Exchange*, **1991**, *9*, 1. Also, see: (b) Horwitz, E. P.; Chiarizia, R.; Dietz, M. L. *Solvent Extraction Ion Exchange* **1992**, *10*, 313. (c) Chiarizia, R.; Horwitz, E. P.; Dietz, M. L. *Solvent Extraction Ion Exchange* **1992**, *10*, 337.

0002-7863/94/1516-10657$04.50/0

as the strontium-90 isotope, together with cesium-137, is the leading source of heat in radioactive waste tanks on the Hanford Nuclear Reservation. Wai and co-workers[21] have also presented a wealth of data on the selective extraction and separation of the lanthanide and actinide elements using ionizable crown ethers. A second practical application of the crown ethers is for treatment of cancerous tissue.[22] Monoclonal antibodies can be designed (by attaching organic chelating agents such as the cryptands or crown ethers) to transport therapeutic doses of radioactivity to the tumor site. By directly attacking the site, this treatment spares normal tissue that is generally destroyed in conventional radiation therapy. Although the present work is far removed from these practical applications, it provides useful data for developing accurate classical force fields. Unlike ab initio methods, force field simulations can efficiently treat dynamical effects of the crown ether and solvent molecules and, hence, may aid in the design of new sequestering agents.[23]

The organization of the paper is as follows: In section II we describe the computational methods and basis sets that were employed. Section III presents the structure of the free 18c6 molecule and the M^+/18c6 complexes together with binding affinities and comparison with crystal structure data. Section IV presents a detailed analysis of the conformational preferences of free and complexed crown ether. This section also discusses the forces (electrostatic, charge transfer, and Pauli repulsions) that influence the binding affinities and the conformations of the various M^+/18c6 complexes. Section V addresses cation selectivity, and section VI concludes with a brief summary.

II. Methods

The 18c6 molecule and its cation complexes are relatively demanding systems to treat by ab initio methods. Each structure consists of a large number of atoms (42 for the uncomplexed crown ether), thereby requiring a large number of basis functions at even modest levels of theory. Furthermore, each structure is highly flexible, a characteristic that complicates the search for minima and significantly extends geometry optimization times. The methods and basis sets employed in this work were therefore selected to provide a reasonably balanced description of the calculated wave functions without overwhelming the available computational resources.

Restricted Hartree–Fock (RHF) wave functions were calculated by the GAUSSIAN 92[24] and GAMESS[25] programs. Due to the floppy nature of these systems, full geometry optimization of each structure was performed using the "tight" gradient convergence threshold of GAUSSIAN 92 or a threshold of 0.000 03 au for GAMESS. These calculations typically required 60 to 100 wave function evaluations to converge the gradients to threshold. Second-order Møller–Plesset perturbation theory (MP2) was applied to several of the optimized structures to determine the influence of electron correlation.

Two basis set levels were employed throughout most of the work. Preliminary calculations were performed with the standard 3-21G basis sets[26] that are readily available for all atoms but cesium. For the latter, we developed a 3-21G-type contraction (specifically, a (18*s*12*p*6*d*)/[7*s*6*p*2*d*] contraction) of Huzinaga's MIDI set.[27] Calculations of 18c6 and its cation complexes at this level consisted of 210–247 basis functions, and geometry optimization using conventional self-consistent-field (SCF) methods generally required 2–3 CPU days on an IBM RS/6000 Model 340.

Higher level calculations were performed with a hybrid basis set that we shall, for brevity, denote "6-31+G*". This set consists of a variety of split valence and effective core potential (ECP) basis sets. For hydrogen, lithium, nitrogen, oxygen, sodium, and sulfur, we used the standard 6-31+G* set and, for carbon, the 6-31G* set.[26] These include six-term *d*-type polarization functions for all atoms other than hydrogen and a diffuse *sp* shell for every heavy atom but carbon. Preliminary calculations of the cation/ether interaction in M^+–$O(CH_3)_2$ revealed that the carbon diffuse functions have little influence on binding energies and structural features. Hence, these functions were neglected in our calculations, decreasing the size of the basis set for 18c6 by 48 functions (a significant number considering the respective n^4 and n^5 formal scalings of the RHF and MP2 methods).

For potassium, rubidium, and cesium, we used a (5*s*5*p*)/[3*s*2*p*] contraction of Hay and Wadt's valence basis sets with ECPs,[28] augmented by six-term *d*-type polarization functions with energy-optimized exponents ($\alpha_d(K) = 0.48$, $\alpha_d(Rb) = 0.24$, and $\alpha_d(Cs) = 0.19$).[29] The outermost $(n - 1)$ shell of core electrons was treated explicitly, the field of the remaining core electrons being described by the ECP. Hay and Wadt[28] demonstrated that basis sets of this form give results comparable to that of all-electron, double-ζ quality sets. The rubidium and cesium ECPs directly incorporate the mass-velocity and one-electron Darwin effects into the potentials and, hence, should approximately treat the dominant relativistic corrections that may contribute importantly to the description of these atoms. All electrons of these metals were correlated in the MP2 calculations as failure to include the $(n - 1)$ shell of core electrons resulted in significant overestimation of the M^+–O distances and, as might be expected, underestimation of the corresponding bond strengths. The carbon and oxygen inner shell electrons were excluded from the MP2 treatment.

Direct SCF calculations at the 6-31+G* level typically consisted of 342–407 basis functions (the latter for the M^+/18c6·2H_2O complexes discussed in section V), and geometry optimization of the M^+/18c6 complexes typically required more than a month of CPU time on the Model 340. The MP2/6-31+G* single-point calculation of Li^+/18c6 required 3.6 CPU h on a Cray C90.

The K^+/18c6 complex was examined with an even larger basis taken from the correlation consistent family of basis sets.[30] A reliable theoretical model of the binding preferences of 18c6 for the alkali metal cations requires an ability to accurately

(21) (a) Tang, T.; Wai, C. M. *Anal. Chem.* **1986**, *58*, 3233. (b) Wai, C. M.; Du, H. S.; Meguro, Y.; Yoshida, Z. *Anal. Sci. (Supplement)* **1991**, *7*, 41. (c) Frazier, R.; Wai, C. M. *Talanta*, **1992**, *39*, 211. (d) Du, H. S.; Wood, D. J.; Elshani, S.; Wai, C. M. *Talanta*, **1993**, *40*, 173.

(22) See, e.g.: Kozak, R. W.; Waldmann, T. A.; Atcher, R. W.; Gansow, O. A. *Trends Biotechnol.* **1985**, *4*, 259.

(23) Hay, B. P.; Rustad, J. R.; Hostetler, C. J. *J. Am. Chem. Soc.* **1993**, *115*, 11158.

(24) GAUSSIAN 92, Rev. A; Frisch, M. J.; Trucks, G. W.; Head-Gordon, M.; Gill, P. M. W.; Wong, M. W.; Foresman, J. B.; Johnson, B. G.; Schlegel, H. B.; Robb, M. A.; Replogle, E. S.; Gomperts, R.; Andres, J. L.; Raghavachari, K.; Binkley, J. S.; Gonzalez, C.; Martin, R. L.; Fox, D. J.; Defrees, D. J.; Baker, J.; Stewart, J. J. P.; Pople, J. A., Gaussian, Inc.: Pittsburgh, PA, 1992.

(25) GAMESS; Schmidt, M. W.; Baldridge, K. K.; Boatz, J. A.; Elbert, S. T.; Gordon, M. S.; Jensen, J. H.; Koseki, S.; Matsunaga, N.; Nguyen, K. A.; Su, S.; Windus, T. L.; Dupuis, M.; Montgomery, J. A., Jr. *J. Comput. Chem.* **1993**, *14*, 1347.

(26) For a comprehensive discussion of the computational methods and basis sets (3-21G, 6-31+G*), see: Hehre, W. J.; Radom, L.; Schleyer, P. v. R.; Pople, J. A. *Ab Initio Molecular Orbital Theory*; Wiley: New York, 1986.

(27) Huzinaga, S.; Andzelm, J.; Klobukowski, M.; Radzio-Andzelm, E.; Sakai, Y.; Tatewaki, H. *Gaussian Basis Sets for Molecular Calculations*; Elsevier: Amsterdam, 1984.

(28) (a) Hay, P. J.; Wadt, W. R. *J. Chem. Phys.* **1985**, *82*, 299. Also, see: (b) Wadt, W. R.; Hay, P. J. *J. Chem. Phys.* **1985**, *82*, 284.

(29) These exponents were optimized for the interaction of the metal cation with a single water molecule, $M^+(H_2O)$.

(30) (a) Dunning, T. H., Jr. *J. Chem. Phys.* **1989**, *90*, 1007. (b) Kendall, R. A.; Dunning, T. H., Jr.; Harrison, R. J. *J. Chem. Phys.* **1992**, *96*, 6796.

describe cation/ether, cation/water, and water/water interactions. In previous work,[31] the aug-cc-pVDZ basis was found to yield binding energies for $(H_2O)_2$ and $M^+(H_2O)$ (M = Li, Na, and K) within 0.1 and 0.6 kcal mol^{-1}, respectively, of the apparent complete basis set limit at the MP2 level of theory. In the present work we examined the performance of these basis sets for describing the cation/ether interaction.

The aug-cc-pVDZ basis set is a (10*s*5*p*2*d*/4*s*2*p*)/[4*s*3*p*2*d*/3*s*2*p*] Gaussian contraction that includes an extra shell of diffuse functions on every atom. The diffuse *s* functions on hydrogen were removed to avoid linear dependency problems in the C_i conformation of 18c6. Test calculations on the water monomer and dimer revealed a negligible effect on geometries, electric moments, polarizabilities, and binding energies as a result of neglecting these basis functions. Because there are currently no correlation consistent sets for potassium, we used a [5*s*4*p*] set from Schäfer[32] augmented with a single five-term *d* function ($\alpha_d = 0.07$). This basis set yielded a total of 628 functions for the K^+/18c6 complex and was the largest attempted in the present study. The single-point RHF/aug-cc-pVDZ calculation required approximately 8 CPU h on a Cray C90 to achieve 10^{-8} convergence in the density.

Binding energies for the M^+/18c6 complexes were calculated at each level of theory. These energies correspond to the gas-phase dissociation energies for the reactions

$$M^+/18c6 \rightarrow M^+ + 18c6 \tag{1}$$

with the uncomplexed 18c6 fragment in the C_i conformation. The full counterpoise correction (CP) of Boys and Bernardi[33] was applied to each binding energy reported here (unless otherwise indicated) to approximately account for basis set superposition error (BSSE). Enthalpy corrections at 298 K were calculated using the standard expressions presented by Del Bene *et al.*[34] Vibrational contributions were evaluated at the RHF/3-21G level and were scaled by the usual factor, 0.9. An estimate of the convergence of the normal mode frequencies and zero point energy with respect to basis set size was determined by re-evaluating the Li^+/18c6 frequencies at the 6-31+G* level.

Wave function analysis was performed by the natural population analysis (NPA)/natural bond orbital (NBO) method[35] of Weinhold and co-workers and by the natural energy decomposition analysis (NEDA).[36] Briefly, NEDA partitions the counterpoise-corrected binding energy for the cation/crown ether interaction into electrostatic (ES), charge transfer (CT), and deformation (DEF) contributions

$$\Delta E = ES + CT + DEF(M^+) + DEF(18c6) + DIS(18c6) \tag{2}$$

assuming a Hamiltonian of the form

$$\hat{\mathcal{H}} = \hat{\mathcal{H}}_{M^+} + \hat{\mathcal{H}}_{18c6} + \hat{\mathcal{H}}_{M^+/18c6} \tag{3}$$

The distortion term of eq 2 (DIS) is the energy penalty arising from the reorganization of the 18c6 nuclear framework from the optimal C_i geometry at infinite separation to that of the complex. The deformation components

$$DEF(M^+) = \langle\psi^{(def)}_{M^+}|\hat{\mathcal{H}}_{M^+}|\psi^{(def)}_{M^+}\rangle - \langle\psi^{(\infty)}_{M^+}|\hat{\mathcal{H}}_{M^+}|\psi^{(\infty)}_{M^+}\rangle \tag{4a}$$

$$DEF(18c6) = \langle\psi^{(def)}_{18c6}|\hat{\mathcal{H}}_{18c6}|\psi^{(def)}_{18c6}\rangle - \langle\psi^{(\infty)}_{18c6}|\hat{\mathcal{H}}_{18c6}|\psi^{(\infty)}_{18c6}\rangle \tag{4b}$$

are positive (destabilizing) quantities associated with the energy required to distort the isolated fragment wave functions $\psi^{(\infty)}$ to those of the complex $\psi^{(def)}$. The latter are single-determinant wave functions constructed from the eigenvectors of fragment blocks of the Fock matrix in the NBO basis. For large separations (generally outside van der Waals' contact), DEF is the energy cost to polarize a fragment charge distribution in the field of its neighbor. At small separations (e.g., for M^+ in the cavity of the crown ether), DEF is principally the energy penalty associated with Pauli repulsions that prevent significant interpenetration of the wave functions $\psi^{(def)}_{M^+}$, $\psi^{(def)}_{18c6}$. The ES component is defined as

$$ES = \langle\psi^{(loc)}_{M^+/18c6}|\hat{\mathcal{H}}|\psi^{(loc)}_{M^+/18c6}\rangle - \langle\psi^{(def)}_{M^+}|\hat{\mathcal{H}}_{M^+}|\psi^{(def)}_{M^+}\rangle - \langle\psi^{(def)}_{18c6}|\hat{\mathcal{H}}_{18c6}|\psi^{(def)}_{18c6}\rangle \tag{5}$$

where

$$\psi^{(loc)}_{M^+/18c6} = A(\psi^{(def)}_{M^+}\psi^{(def)}_{18c6}) \tag{6}$$

and *A* is the antisymmetrizer. Equation 5 differs in two respects from more traditional treatments of electrostatics.[37] First, electrostatic interaction is typically defined as the interaction of two unpolarized wave functions $\psi^{(\infty)}$, whereas it is expressed here in terms of the distorted forms $\psi^{(def)}$. ES therefore contains polarization contributions that arise from the interaction of permanent electric moments of one fragment with the induced moments of its neighbor. Second, traditional treatments generally evaluate the electrostatic interaction using a Hartree product of fragment wave functions, thereby neglecting interfragment exchange effects. On the other hand, the wave function of eq 6 is a fully antisymmetrized wave function so that ES contains an exchange contribution. Previous work[10] has suggested however that exchange effects are negligible for interactions having minimal covalent bonding character (as in the M^+···18c6 interaction) so that ES is almost entirely the "classical" electrostatic interaction of the fragment wave functions. Finally, the CT component is given by

$$CT = \langle\psi_{M^+/18c6}|\hat{\mathcal{H}}|\psi_{M^+/18c6}\rangle - \langle\psi^{(loc)}_{M^+/18c6}|\hat{\mathcal{H}}|\psi^{(loc)}_{M^+/18c6}\rangle \tag{7}$$

where $\psi_{M^+/18c6}$ is the variationally optimized wave function of the complex. CT stabilizes the complex, allowing electron density of the wave functions $\psi^{(def)}$ to delocalize over the fragments.

III. Geometries and Binding Affinities

A. Uncomplexed 18c6. Molecular dynamics[8,10,12] and Monte Carlo simulations[14,15] suggest that 18c6 is extremely flexible, sampling dozens of low energy conformations at room

(31) (a) Feller, D. *J. Chem. Phys.* **1992**, *96*, 610. (b) Feller, D.; Glendening, E. D.; Kendall, R. A.; Peterson, K. A. *J. Chem. Phys.* **1994**, *100*, 4981. (c) Feller, D.; Woon, D. E.; Glendening, E. D., to be published.

(32) Schäfer, A.; Horn, H.; Ahlrichs, R. *J. Chem. Phys.* **1992**, *97*, 2571. Details of the potassium basis sets used in this work are available from the authors upon request.

(33) Boys, S. F.; Bernardi, F. *Mol. Phys.* **1970**, *19*, 553.

(34) Del Bene, J. E.; Mettee, H. D.; Frisch, M. J.; Luke, B. T.; Pople, J. A. *J. Phys. Chem.* **1983**, *87*, 3279.

(35) (a) Reed, A. E.; Weinstock, R. B.; Weinhold, F. *J. Chem. Phys.* **1985**, *83*, 735. (b) Reed, A. E.; Curtiss, L. A.; Weinhold, F. *Chem. Rev.* **1988**, *88*, 899. (c) NBO 4.0; Glendening, E. D.; Badenhoop, J. K.; Reed, A. E.; Carpenter, J. E.; Weinhold, F. Theoretical Chemistry Institute, University of Wisconsin, Madison, WI, 1994.

(36) Glendening, E. D.; Streitwieser, A. *J. Chem. Phys.* **1994**, *100*, 2900.

(37) Morokuma, K. *Acc. Chem. Res.* **1977**, *10*, 294, and references therein.

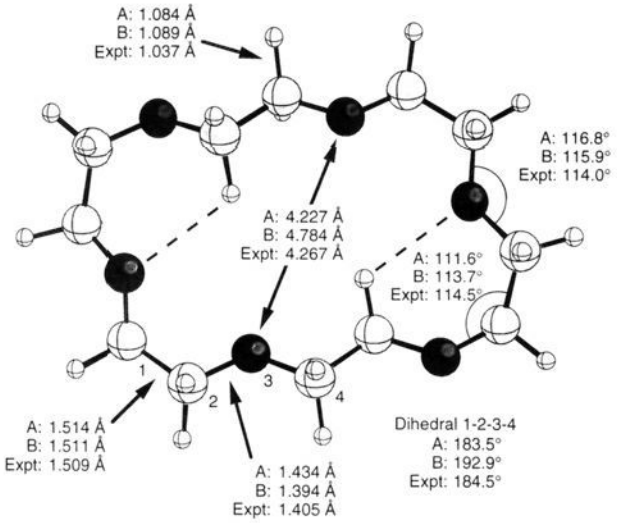

Figure 1. C_i conformation of 18c6 with the two 1,5 CH···O interactions highlighted by dashed lines. Selected geometrical parameters are listed for the RHF/3-21G (A) and RHF/6-31+G* (B) levels of theory together with experimentally determined values.

temperature in both gas- and condensed-phases. Of these conformations, two are particularly important, those of apparent lowest energy (C_i) and highest symmetry (D_{3d}). The C_i form (Figure 1) has four of its six ether oxygens directed inward from the ether backbone with the other two directed outward. This conformation is observed in the X-ray analysis[38] of crystalline 18c6 and is the most frequently sampled conformation in both gas-phase simulations[10] and simulations of 18c6 in apolar solvents.[14] Molecular mechanics treatments[6] indicate that the C_i structure is several kcal mol^{-1} more stable than all other conformations, stabilized in part by two transannular 1,5 CH···O interactions, highlighted by dashed lines in Figure 1. The D_{3d} structure (Figure 2), with each of its oxygen centers directed inward from the ether backbone, forms a nucleophilic cavity for interaction with guest molecules or ions. Proton and carbon-13 NMR data[39] and condensed-phase simulations[10] suggest that the D_{3d} conformation is the dominant one in polar solvents.

Both conformations were optimized at the RHF/3-21G and RHF/6-31+G* levels. A summary of the geometrical features is given in Table 1 together with experimentally determined values for the C_i crystal structure, and selected structural details are shown in Figures 1 and 2. Although the interactions of 18c6 with neighboring solvent and crown ether molecules in the crystal can strongly influence the observed structure, we find the crystal structure to be remarkably similar to the gas-phase C_i conformation. Bond lengths typically agree to within 0.01 Å, except for the CO bonds at 3-21G that appear to be too long by ca. 0.03−0.04 Å. The transannular O···O distance is rather long at the 6-31+G* level (4.784 Å), significantly longer than either the 3-21G optimized or experimental distances (4.227 and 4.267 Å, respectively). However, this feature depends sensitively on the bond lengths and angles about the ring and possibly on packing forces in crystalline 18c6 so that it is unlikely that the discrepancy (calculated vs crystal) reflects a significant inadequacy in the RHF/6-31+G* method. Reoptimization of the C_i conformation with a basis set containing polarization functions on all atoms (6-31G**)[26] reveals differences of less than 0.01 Å in all bond lengths, although the transannular O···O distance shortens slightly to 4.660 Å.

(38) Dunitz, J. D.; Dobler, M.; Seiler, P.; Phizackerley, R. P. *Acta. Crystallogr.* **1974**, *B30*, 2733 and references therein.
(39) Live, D.; Chan, S. I. *J. Am. Chem. Soc.* **1976**, *98*, 3769.

The calculated bond angles are also reasonably similar to those observed in the crystal structure. The COC bond angles (e.g., 115.7−116.9° at 6-31+G*) are somewhat larger than tetrahedral, as observed experimentally (113.3−114.0°). The calculated D_{3d} structure is more "flat" than the DFT structure reported by Ha and Chakraborty.[18] We calculate an OCCO dihedral angle of 75.4° at 6-31+G*, significantly less than their optimized angle of 97°. The OCCO dihedral angle is, on the other hand, the only geometrical parameter optimized in their calculations, since all other bond lengths and bond angles were constrained to the average values determined from various crystal structures.

The C_i conformation is 4.4 kcal mol^{-1} more stable than the D_{3d} at RHF/6-31+G* (5.4 kcal mol^{-1} at the MP2 level) in fair agreement with molecular mechanical force field results. Howard *et al.*[8] calculated an energy difference of 1.1 kcal mol^{-1} using a polarizable variant of the AMBER force field, and Sun and Kollman[12] more recently reported an energy difference of 2.0 kcal mol^{-1} using related methods. In contrast, RHF/3-21G strongly overestimates the relative stability of the C_i structure, suggesting that it is 19.6 kcal mol^{-1} more stable than the D_{3d} form.

B. Li^+/18c6 and Na^+/18c6. Two structures were calculated for each of the Li^+/18c6 and Na^+/18c6 complexes, and details of the optimized geometrical parameters are given in Table 1. One of these structures corresponds to the "open" D_{3d} conformation described above with the metal cation residing at the center of the cavity. Since Li^+ and Na^+ cations are rather small and unable to fully occupy the cavity, it seems unlikely that these open structures are stable (that is, correspond to minima on the potential energy surface). This was confirmed by normal mode analysis which revealed four and two negative eigenvalues of the RHF/3-21G force constant matrix for Li^+/18c6 and Na^+/18c6, respectively. We therefore calculated for each complex a structure of lower symmetry in which the ether backbone has collapsed about the cation center.

For Li^+/18c6, we optimized a "folded" structure of approximate S_6 symmetry that almost fully encloses the cation center (see Figure 3). The ether oxygens coordinate the metal in a distorted octahedral arrangement with Li^+···O distances that are significantly shorter than those of the D_{3d} form (2.196 vs 2.718 Å at RHF/6-31+G*). The RHF/6-31+G* binding energy is −89.1 kcal mol^{-1} compared to −86.8 kcal mol^{-1} for D_{3d}, suggesting that the relative stability of the S_6 form is only −2.3 kcal mol^{-1}. While this structure is the more stable of the two that we optimized, it is unlikely that it will be frequently sampled in polar solvents. The dipole moment of the complex is negligible, and the folded ether conformation effectively prohibits any direct coordination of the metal by the solvent. Harmonic vibrational frequencies were evaluated for this conformation at the RHF/6-31+G* level. The resulting zero point energy only differed by 1.0 kcal mol^{-1} from that determined with the smaller 3-21G basis. Hence, it appears that the vibrational corrections are adequately represented at the 3-21G level.

We also obtained the asymmetrical (C_1) geometry of the Na^+/18c6 complex shown in Figure 4. At RHF/3-21G, this structure is 4.5 kcal mol^{-1} more stable than the D_{3d} form. However, the 6-31+G* optimized structure is less stable than D_{3d} by 2.9 and 2.5 kcal mol^{-1} at the RHF and MP2 levels, respectively. We obtained the 3-21G C_1 geometry starting from an initial structure that was slightly distorted from D_{3d} symmetry. The 3-21G optimized structure was subsequently used as the initial guess geometry in the 6-31+G* optimization. Several attempts to identify a low energy C_1 structure failed with the 6-31+G* basis.

Table 1. Summary of Optimized Geometrical Parameters for Free 18c6 and Its Complexes with the Alkali Metals[a]

		RHF/3-21G			RHF/6-31+G*			expt[b]		
	sym	min	mean	max	min	mean	max	min	mean	max
					CC Bond Lengths					
free	C_i	1.514	1.516	1.519	1.512	1.514	1.517	1.505	1.507	1.509
	D_{3d}	1.518	1.518	1.518	1.511	1.511	1.511			
Li^+	S_6	1.524	1.524	1.524	1.522	1.522	1.522			
	D_{3d}	1.503	1.503	1.503	1.502	1.502	1.502			
Na^+	C_1	1.513	1.521	1.530	1.508	1.513	1.519	1.491	1.502	1.511
	D_{3d}	1.505	1.505	1.505	1.504	1.504	1.504			
K^+	D_{3d}	1.512	1.512	1.512	1.510	1.510	1.510	1.497	1.504	1.507
Rb^+	C_{3v}				1.512	1.512	1.512	1.476	1.489	1.500
	D_{3d}	1.517	1.517	1.517	1.516	1.516	1.516			
Cs^+	C_{3v}	1.518	1.518	1.518	1.512	1.512	1.512	1.464	1.475	1.491
	D_{3d}	1.525	1.525	1.525	1.525	1.525	1.525			
					CO Bond Lengths					
free	C_i	1.430	1.436	1.447	1.394	1.398	1.405	1.403	1.410	1.426
	D_{3d}	1.433	1.433	1.433	1.393	1.393	1.393			
Li^+	S_6	1.448	1.450	1.452	1.406	1.407	1.409			
	D_{3d}	1.439	1.439	1.439	1.402	1.402	1.402			
Na^+	C_1	1.439	1.447	1.454	1.402	1.406	1.412	1.410	1.423	1.437
	D_{3d}	1.440	1.440	1.440	1.403	1.403	1.403			
K^+	D_{3d}	1.442	1.442	1.442	1.405	1.405	1.405	1.414	1.418	1.424
Rb^+	C_{3v}				1.403	1.404	1.405	1.401	1.414	1.435
	D_{3d}	1.444	1.444	1.444	1.407	1.407	1.407			
Cs^+	C_{3v}	1.442	1.443	1.443	1.402	1.403	1.404	1.392	1.418	1.445
	D_{3d}	1.446	1.446	1.446	1.410	1.410	1.410			
					M–O Distances					
free[c]	D_{3d}	2.973	2.973	2.973	2.901	2.901	2.901			
Li^+	S_6	2.214	2.214	2.214	2.196	2.197	2.197			
	D_{3d}	2.659	2.659	2.659	2.718	2.718	2.718			
Na^+	C_1	2.266	2.309	2.349	2.417	2.484	2.612	2.452	2.548	2.623
	D_{3d}	2.710	2.710	2.710	2.738	2.738	2.738			
K^+	D_{3d}	2.802	2.802	2.802	2.809	2.809	2.809	2.770	2.805	2.833
Rb^+	C_{3v}				2.982	2.984	2.986	2.929	3.024	3.146
	D_{3d}	2.865	2.865	2.865	2.875	2.875	2.875			
Cs^+	C_{3v}	3.061	3.077	3.093	3.212	3.216	3.220	3.035	3.146	3.274
	D_{3d}	2.954	2.954	2.954	2.966	2.966	2.966			
					COC Bond Angles					
free	C_i	114.7	116.3	117.3	115.7	116.1	116.9	113.3	113.5	114.0
	D_{3d}	115.0	115.0	115.0	114.5	114.5	114.5			
Li^+	S_6	116.9	116.9	116.9	118.3	118.3	118.3			
	D_{3d}	114.4	114.4	114.4	113.4	113.4	113.4			
Na^+	C_1	115.1	117.2	119.0	113.9	116.5	118.4	111.4	113.3	116.5
	D_{3d}	114.1	114.1	114.1	113.6	113.6	113.6			
K^+	D_{3d}	114.6	114.6	114.6	114.4	114.4	114.4	111.6	112.2	112.9
Rb^+	C_{3v}				113.8	114.7	115.6	110.9	112.3	114.1
	D_{3d}	114.9	114.9	114.9	115.1	115.1	115.1			
Cs^+	C_{3v}	113.8	115.1	116.3	113.5	114.5	115.5	111.3	113.0	113.9
	D_{3d}	115.9	115.9	115.9	116.2	116.2	116.2			
					OCC Bond Angles					
free	C_i	103.7	107.3	111.6	107.2	109.3	113.7	106.4	109.8	114.6
	D_{3d}	107.9	107.9	107.9	109.8	109.8	109.8			
Li^+	S_6	108.3	108.7	109.1	109.7	110.1	110.6			
	D_{3d}	105.6	105.6	105.6	108.3	108.3	108.3			
Na^+	C_1	105.4	108.1	111.4	106.8	109.1	111.9	106.0	109.2	113.6
	D_{3d}	106.3	106.3	106.3	108.6	108.6	108.6			
K^+	D_{3d}	107.5	107.5	107.5	109.5	109.5	109.5	107.5	108.5	109.4
Rb^+	C_{3v}				109.3	109.8	110.3	108.6	109.4	110.5
	D_{3d}	108.2	108.2	108.2	110.3	110.3	110.3			
Cs^+	C_{3v}	107.8	108.5	109.1	109.4	109.9	110.4	108.6	109.8	111.0
	D_{3d}	109.0	109.0	109.0	111.1	111.1	111.1			
					OCCO Dihedral Angles					
free	D_{3d}	83.2	83.2	83.2	75.4	75.4	75.4			
Li^+	S_6	45.5	45.5	45.5	46.1	46.1	46.1			
	D_{3d}	59.5	59.5	59.5	59.0	59.0	59.0			
Na^+	C_1	45.6	54.5	64.5	51.3	55.1	57.3			
	D_{3d}	61.5	61.5	61.5	60.0	60.0	60.0			
K^+	D_{3d}	65.5	65.5	65.5	63.8	63.8	63.8			
Rb^+	C_{3v}				65.3	65.3	65.3			
	D_{3d}	69.0	69.0	69.0	67.7	67.7	67.7			
Cs^+	C_{3v}	70.5	70.5	70.5	65.9	65.9	65.9			
	D_{3d}	74.9	74.9	74.9	73.9	73.9	73.9			

[a] Distances in Å, angles in deg. [b] Dunitz, Dobler, Seiler, and Phizackerley, ref 38. [c] One-half the O–O distance in the D_{3d} 18c6 structure.

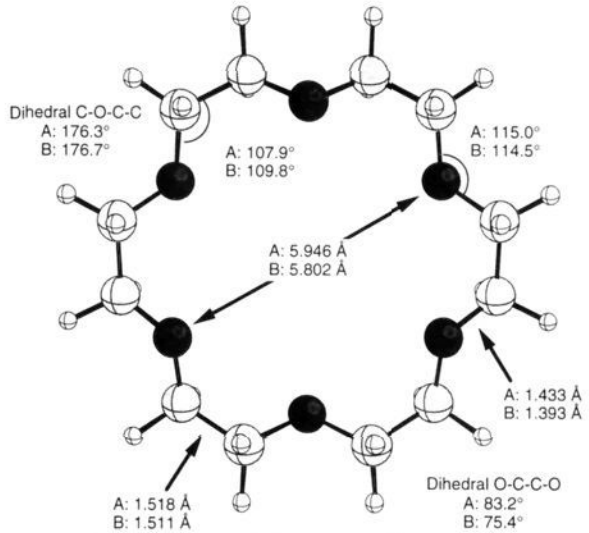

Figure 2. D_{3d} conformation of 18c6. Selected geometrical parameters are listed for the RHF/3-21G (A) and RHF/6-31+G* (B) levels of theory.

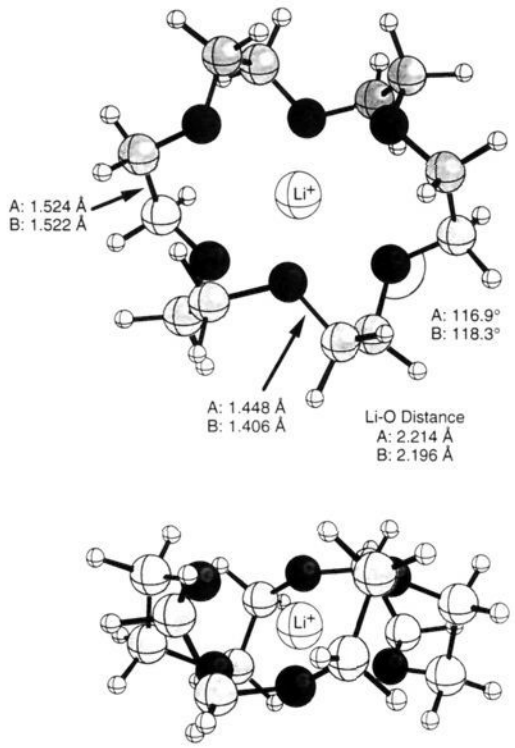

Figure 3. Top and side views of the S_6 conformation of Li^+/18c6. Selected geometrical parameters are listed for the RHF/3-21G (A) and RHF/6-31+G* (B) levels of theory.

In each calculation the geometry reverted to D_{3d} symmetry, thereby suggesting that this conformation is a stable equilibrium structure rather than a saddle point at the larger basis set level. The D_{3d} conformation was also observed in a crystal structure of Na^+/18c6.[40]

Figure 5 shows the CP corrected binding energies for Li^+/18c6 and Na^+/18c6 at the three levels of theory employed together with the uncorrected RHF/3-21G energies. The binding energies for the K^+, Rb^+, and Cs^+ complexes are also shown and will be discussed in more detail later. Several general

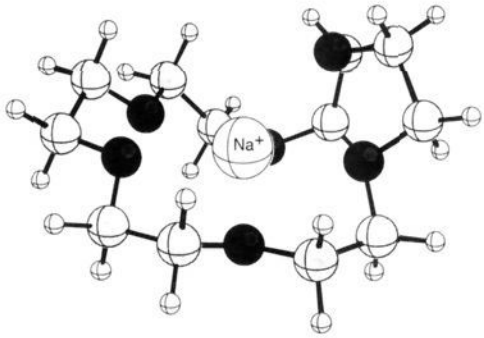

Figure 4. C_1 conformation of Na^+/18c6.

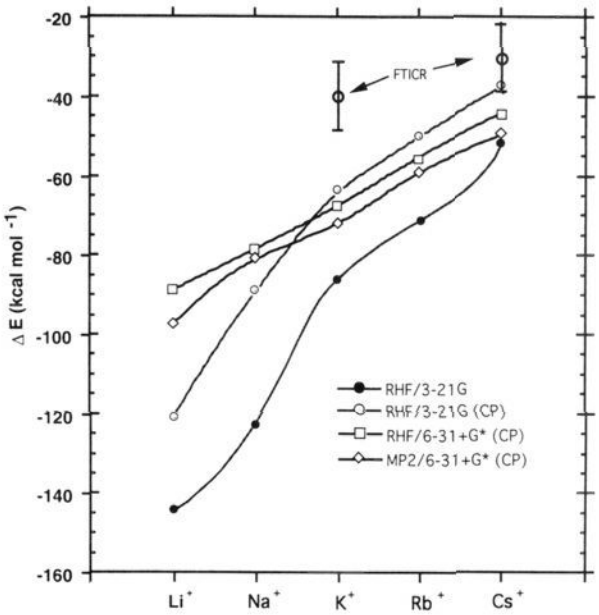

Figure 5. Binding energies of the M^+/18c6 complexes as a function of cation type and level of theory. Energies are plotted for the lowest energy conformations only. All energies are counterpoise (CP) corrected except for the RHF/3-21G curve (solid circles). The FTICR (experimental) values are reported in ref 41.

observations can be made that apply equally well to all M^+/18c6 complexes. First, all levels of theory predict that the binding affinity of 18c6 decreases with increasing cation size. This is particularly noteworthy as it suggests that gas-phase 18c6 will most strongly bind Li^+ rather than K^+. (We return to this issue in section V.) Second, cation/crown ether interactions appear to be inadequately described at the RHF/3-21G level. Comparison of the CP corrected binding energies evaluated at this level with the most reliable values that we report (MP2/6-31+G*) suggests that RHF/3-21G strongly overestimates the binding strength for the Li^+ and Na^+ complexes and underestimates the binding strength for the K^+, Rb^+, and Cs^+ complexes. Furthermore, BSSE at the RHF/3-21G level is quite large in comparison to that of the more extended basis set methods. For example, the CP corrections for Na^+/18c6 are -34.1, -3.8, and -13.7 kcal mol^{-1} at RHF/3-21G, RHF/6-31+G*, and MP2/6-31+G*, respectively. Corrections of similar magnitude were evaluated for the other complexes. Finally, electron correlation tends to stabilize the cation

(40) Bailey, S. I.; Engelhardt, L. M.; Leung, W.-P.; Raston, C. L.; Ritchie, I. M.; White, A. H. *J. Chem. Soc., Dalton Trans.* **1985**, 1747.

(41) (a) Katritzky, A. R.; Malhotra, N.; Ramanathan, R.; Kemerait, R. C., Jr.; Zimmerman, J. A.; Eyler, J. R. *Rapid Commun. Mass Spectrosc.* **1992**, *6*, 25. Additional details of the experimental method are given: (b) Katritzky, A. R.; Watson, C. H.; Dega-Szafran, Z.; Eyler, J. R. *J. Am. Chem. Soc.* **1990**, *112*, 2471.

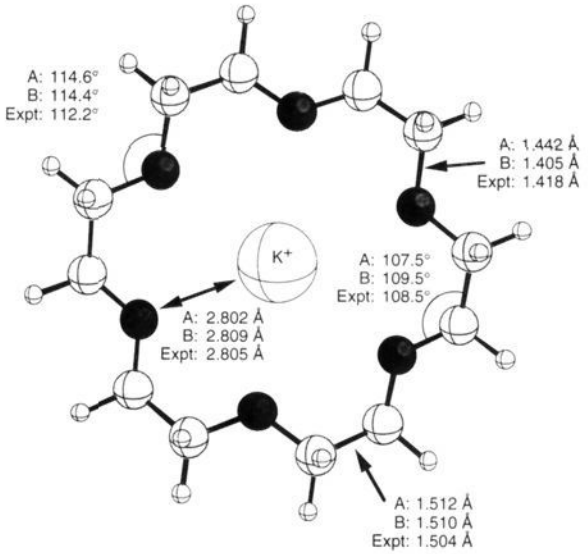

Figure 6. D_{3d} conformation of K^+/18c6. Selected geometrical parameters are listed for the RHF/3-21G (A) and RHF/6-31+G* (B) levels of theory together with experimentally determined average values.

complexes, increasing the binding affinity. For the S_6 conformation of Li^+/18c6, this effect is rather large, strengthening the binding energy by -8.4 kcal mol^{-1} from -89.1 (RHF) to -97.5 (MP2) kcal mol^{-1}. The correlation effects in the other complexes are somewhat smaller, ranging from -1.7 to -5.0 kcal mol^{-1}.

C. K^+/18c6. The optimized D_{3d} conformation of the K^+/18c6 complex is shown in Figure 6. Molecular dynamics simulations[9,11,13] and the crystal structure[38] both suggest that this conformation is more stable than any alternative, and normal mode analysis at the RHF/3-21G level indeed reveals that the structure corresponds to an energy minimum. The geometrical parameters listed in Table 1 show that the calculated 3-21G and 6-31+G* geometries are nearly identical to the crystal structure, except for the 3-21G CO bonds. As in uncomplexed 18c6, these bonds appear to be somewhat too long.

Our best estimate for the binding enthalpy for the K^+/18c6 complex (-71.5 kcal mol^{-1} at MP2/6-31+G* and 298 K) is significantly larger than the only available experimental value. Katritzky *et al.*[41] reported a binding enthalpy (appearance energy) of only -40 ± 8 kcal mol^{-1} at 350 K in a Fourier-transform ion cyclotron resonance (FTICR) study of the dissociation of various cation/crown ether complexes (cf. Figure 5). Temperature corrections cannot account for this large difference. In fact, we calculate a binding enthalpy of -71.8 kcal mol^{-1} at 350 K, 0.3 kcal mol^{-1} *stronger* than the 298 K value. The RHF/3-21G binding enthalpy (-63.4 kcal mol^{-1}) is somewhat closer to the experimental value, but the large CP correction (-22.6 kcal mol^{-1}) at this basis set level undermines its reliability. Extending the 3-21G calculations to 6-31+G* and the level of theory from RHF to MP2 tends to strengthen the cation/crown ether interaction.

To assess our ability to accurately compute the K^+/18c6 interaction energy, we carried out a series of high-level calculations with the correlation consistent basis sets on the prototype K^+/dimethyl ether system. The structures of this complex and the uncomplexed dimethyl ether were optimized with the aug-cc-pVDZ and aug-cc-pVTZ basis sets[30] at both the RHF and MP2 levels of theory. The potassium basis sets were derived from the [5*s*4*p*1*d*] set of Schäfer *et al.*[32] described in section II, but additional functions were added to permit improved correlation of the (3*s*3*p*) electrons. This resulted in a [6*s*5*p*2*d*] potassium set being used with the aug-cc-pVDZ basis on hydrogen, carbon, and oxygen and an [8*s*7*p*4*d*2*f*] set being used in conjunction with the aug-cc-pVTZ basis. At over 570 basis functions, calculations with the next larger correlation consistent basis set, aug-cc-pVQZ, were judged to be prohibitively expensive.

As can be seen in Figure 7, where the results of cc-pVxZ and diffuse-function-augmented sets are plotted as a function of basis set size, the MP2/6-31+G* counterpoise corrected

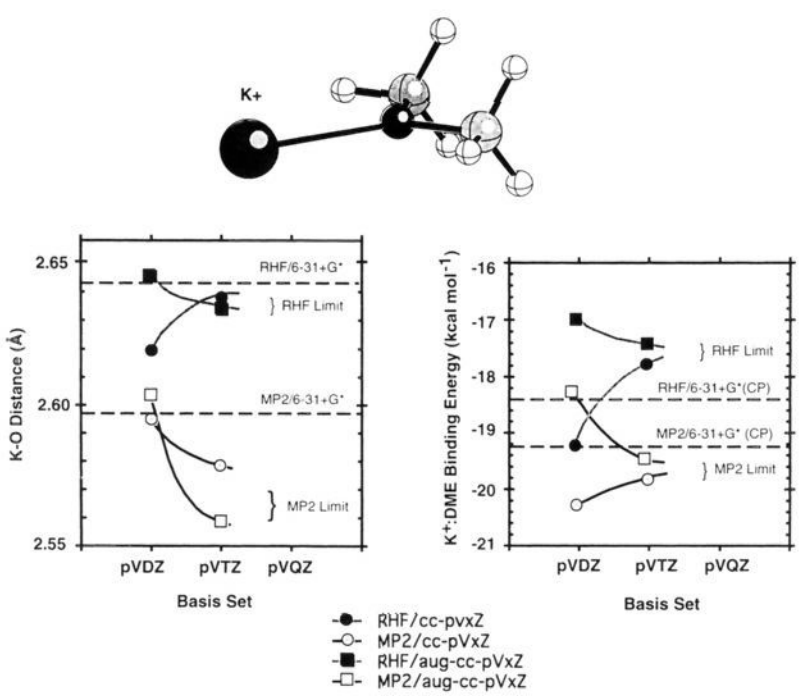

Figure 7. Dependence of the K^+–O distance and binding energy for K^+/dimethyl ether (DME) on basis set and level of theory. A rough estimate of the RHF and MP2 complete basis set limits are provided for comparison with the 6-31+G* values. The 6-31+G* binding energies are counterpoise (CP) corrected, while the correlation consistent values are not.

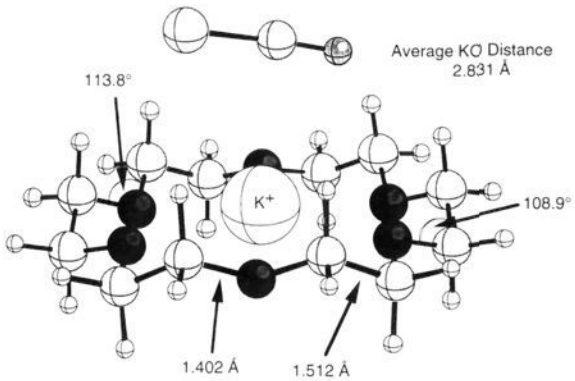

Figure 8. RHF/6-31+G* optimized structure for the KSCN complex of 18c6.

binding energy is in good agreement with the apparent basis set limit. The K^+···O distance predicted by the 6-31+G* basis appears to be slightly longer than the basis set limit. On the basis of these findings, we conclude that the highest computational level that we could afford to apply to the M^+/18c6 complexes should be capable of predicting binding energies with a rough accuracy of $\pm 5-7$ kcal mol^{-1}. Thus, it remains unclear how to reconcile the 30 kcal mol^{-1} difference between the calculated and experimental binding enthalpies.

We also optimized the KSCN complex of 18c6 (RHF/6-31+G*, shown in Figure 8) to examine the influence of a counterion (the thiocyanate ion in this case) on structure and for direct comparison with the crystal structure reported by Dunitz *et al.*[38] The crown ether geometry is only marginally perturbed by the counterion. On average, the bond lengths are essentially identical to those obtained in the absence of the counterion, while the bond angles change by 2° at most. The K^+···O distances are lengthened somewhat (~0.03 Å), and the K^+ cation is displaced from the crown ether center of mass by 0.24 Å. All geometrical parameters compare quite favorably with the crystal structure. Perhaps the most interesting feature of the optimized structure is the orientation of the SCN^- ion. Whereas coordination occurs at either sulfur or nitrogen in the crystal, K^+ appears to coordinate the carbon in the optimized geometry (K^+···C = 3.101 Å, K^+···N = 3.199 Å). RHF/6-31+G* calculation of the KSCN complex (in the absence of 18c6) also gave a T-shaped geometry, K^+ coordinating carbon. Direct comparison of the calculated and crystal structures is, however, somewhat misleading as the SCN^- ion simultaneously coordinates two adjacent K^+/18c6 complexes in the crystal.

D. Rb^+/18c6 and Cs^+/18c6. The Rb^+ and Cs^+ cations are too large to fit into the cavity of 18c6 without significantly straining the ether backbone. Thus, we optimized two geometries for each of these complexes, the high symmetry D_{3d} structure in which the cation is forced to occupy the cavity and a lower symmetry C_{3v} structure in which the cation sits some distance outside. Details of these geometries are given in Table 1, and the C_{3v} structures are shown in Figures 9 and 10. Note that the D_{3d} structure is the most stable geometry for Rb^+/18c6 at the RHF/3-21G level. An attempt to identify the C_{3v} structure failed as the cation returned to the cavity during optimization. At RHF/6-31+G*, the Rb^+ and Cs^+ cations are displaced from the 18c6 center of mass of the C_{3v} structures by 1.01 and 1.60 Å, respectively. Comparison of the 3-21G and 6-31+G* optimized geometries reveals several significant differences. Again, the 3-21G CO bond lengths are 0.04−0.05 Å longer than at 6-31+G*, and the M^+···O distances in the C_{3v} structures are 0.12−0.15 Å shorter at 3-21G than 6-31+G*. The 3-21G M^+···O distances are probably spuriously small due to large

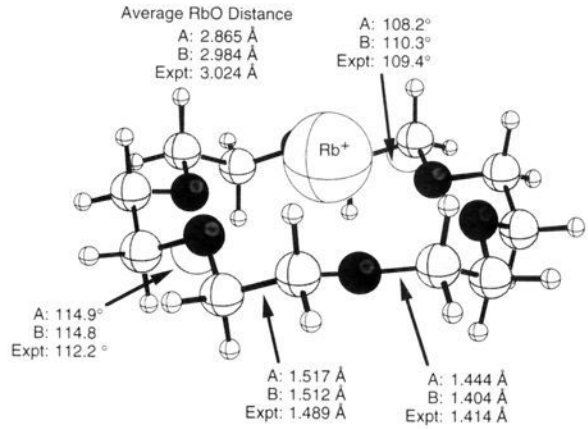

Figure 9. C_{3v} conformation of Rb^+/18c6. Selected geometrical parameters are listed for the RHF/3-21G (A) and RHF/6-31+G* (B) levels of theory together with experimentally determined average values.

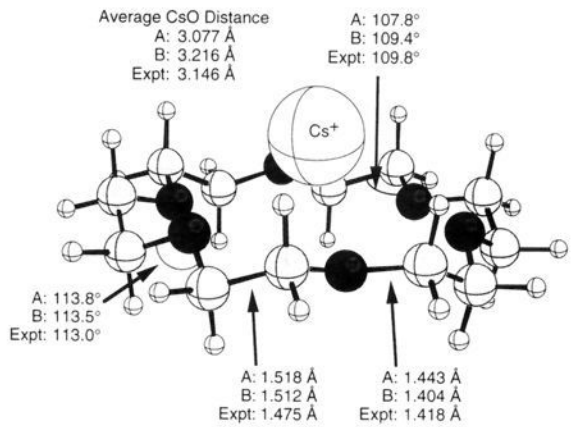

Figure 10. C_{3v} conformation of Cs^+/18c6. Selected geometrical parameters are listed for the RHF/3-21G (A) and RHF/6-31+G* (B) levels of theory together with experimentally determined average values.

BSSE that favors short distances. CP corrections are −20.9 and −1.1 kcal mol^{-1} for Rb^+/18c6 and −16.4 and −1.1 kcal mol^{-1} with Cs^+/18c6 for the 3-21G and 6-31+G* basis sets, respectively.

The RHF/6-31+G* optimized geometries generally resemble the crystal structures. The calculated M^+···O distances and CO bond lengths lie within the range of measured values, and the COC and OCC bond angles differ by a few degrees at most. A larger disparity appears for the CC bond lengths. While the bond lengths that we calculate for Rb^+/18c6 and Cs^+/18c6 are nearly identical to those calculated for the lighter alkali metal complexes, they are 0.02−0.04 Å longer than the average CC bond determined in the crystal structure. Dunitz *et al.* also recognized the short CC bond lengths in their Rb^+/18c6 and Cs^+/18c6 crystal structures.[38] They argued that the apparent bond shortening in the crystal was a spurious effect from the inadequate treatment of thermal motions in the analysis of their data.

The affinity of 18c6 for Rb^+ and Cs^+ cations is less than that for Li^+, Na^+, and K^+, as shown in Figure 5. At the MP2/6-31+G* level we evaluate binding enthalpies of −58.1 and −48.7 kcal mol^{-1} for the Rb^+ and Cs^+ complexes, respectively. Since no C_{3v} structure was obtained for Rb^+/18c6 with the 3-21G basis set, the zero point energy and temperature dependent vibrational corrections for the Rb^+ complexes were obtained from the D_{3d} structure. Katritzky *et al.*[41] reported a binding enthalpy for Cs^+/18c6 of -32 ± 8 kcal mol^{-1}. As with K^+/18c6, this value is much weaker than our MP2/6-31+G*

Table 2. Total Energies, Binding Energies, and Binding Enthalpies of Free and Complexed 18c6[a]

	sym	method	energy	ΔE^b	ΔH^{298} [b]
free	C_i	RHF/3-21G	−912.410 26		
		RHF/6-31+G*	−917.500 35		
		MP2/6-31+G*	−920.127 97		
		RHF/aug-cc-pVDZ	−917.611 04		
	D_{3d}	RHF/3-21G	−912.379 08		
		RHF/6-31+G*	−917.493 31		
		MP2/6-31+G*	−920.119 42		
Li^+	S_6	RHF/3-21G	−919.827 52	−121.0	−118.9
		RHF/6-31+G*	−924.884 77	−89.1	−86.9
		MP2/6-31+G*	−927.534 25	−97.5	−95.4
	D_{3d}	RHF/3-21G	−919.771 56	−90.9	
		RHF/6-31+G*	−924.877 49	−86.8	
Na^+	C_1	RHF/3-21G	−1073.280 09	−88.9	−88.3
		RHF/6-31+G*	−1079.291 26	−78.8	−78.2
		MP2/6-31+G*	−1081.937 95	−80.9	−80.3
	D_{3d}	RHF/3-21G	−1073.257 04	−84.4	
		RHF/6-31+G*	−1079.293 75	−81.7	
		MP2/6-31+G*	−1081.933 30	−83.4	
K^+	D_{3d}	RHF/3-21G	−1508.554 69	−63.9	−63.4
		RHF/6-31+G*	−945.316 31	−68.1	−67.6
		MP2/6-31+G*	−948.027 53	−72.0	−71.5
		RHF/aug-cc-pVDZ	−1516.723 07	−62.6	
Rb^+	C_{3v}	RHF/6-31+G*	−941.033 61	−55.2	−54.1[c]
		MP2/6-31+G*	−943.706 40	−59.2	−58.1[c]
	D_{3d}	RHF/3-21G	−3837.099 95	−50.1	−49.1
		RHF/6-31+G*	−941.030 17	−52.8	−51.8
Cs^+	C_{3v}	RHF/3-21G	−8442.913 90	−35.0	−35.1
		RHF/6-31+G*	−937.052 07	−44.6	−43.7
		MP2/6-31+G*	−939.730 63	−49.6	−48.7
	D_{3d}	RHF/3-21G	−8442.908 81	−29.9	
		RHF/6-31+G*	−937.030 04	−30.4	

[a] Total energies in au. Binding energies and enthalpies in kcal mol^{-1}. Binding energies evaluated relative to free metal cation and 18c6 (C_i). Enthalpy corrections determined using the RHF/3-21G harmonic vibrational frequencies. RHF energies for the 3-21G and 6-31+G* basis sets evaluated at their optimal geometries. MP2/6-31+G* and aug-cc-pVDZ energies calculated at the RHF/6-31+G* geometries. [b] Including the counterpoise correction for basis set superposition error for all entries except aug-cc-pVDZ. [c] Enthalpy corrections calculated using the harmonic frequencies of the D_{3d} Rb^+/18c6 structure.

estimate. Finally, the barrier for Rb^+ and Cs^+ cations to move from their optimal position in the C_{3v} structure through the cavity can be evaluated as a difference for binding energies (D_{3d}−C_{3v}). At the RHF/6-31+G* level these barriers are 2.4 and 14.2 kcal mol^{-1} for Rb^+/18c6 and Cs^+/18c6, respectively.

IV. Conformational Preferences and Cation/Crown Ether Interactions

To investigate the conformational preferences of 18c6 and its interaction with the alkali metal cations in more detail, we analyzed the RHF/6-31+G* wave functions with the NPA/NBO and NEDA methods. Atomic and fragment charges and CO bond ionicities for the free and complexed 18c6 are listed in Table 3, and details of NEDA are given in Table 4.

It is generally argued that the conformational preference of 18c6 is a direct result of stabilizing 1,5 CH···O interactions in the C_i form and destabilizing O···O interactions in the D_{3d}. NPA and NBO analysis both provide evidence of electrostatic/polarization forces in the C_i structure. The hydrogen centers involved in the CH···O interactions (cf Figure 1) have slightly greater charge (+0.217) than any of the other hydrogens in the molecule (ranging from +0.181 to +0.208).[42] Furthermore, the percent ionic character of the two CH bonding NBOs, 22.7% in the sense C^-H^+, is somewhat greater than that of the other

Table 3. Atomic and Fragment Charges and Percentage CO Bond Ionicity for 18c6 and Its Alkali Metal Complexes[a]

	sym	$q(M^+)$	$q(O)$	$q(CH_2)$	$\Delta q(CH_2)^b$	C^+O^-
free	C_i		−0.710	0.355	0.000	38.40
	D_{3d}		−0.694	0.347	−0.008	37.66
Li^+	S_6	0.901	−0.743	0.380	0.025	39.90
	D_{3d}	0.939	−0.731	0.371	0.016	39.26
Na^+	C_1	0.928	−0.739	0.375	0.020	39.58
	D_{3d}	0.943	−0.732	0.371	0.016	39.28
K^+	D_{3d}	0.953	−0.734	0.371	0.016	39.28
Rb^+	C_{3v}	0.958	−0.730	0.368	0.013	39.11
	D_{3d}	0.952	−0.733	0.371	0.016	39.24
Cs^+	C_{3v}	0.969	−0.727	0.366	0.011	38.94
	D_{3d}	0.960	−0.735	0.371	0.016	39.24

[a] RHF/6-31+G* values. Values averaged over atomic or fragment units for low symmetry cases. [b] Average charge of the methylene group relative to that of free 18c6 (C_i).

Table 4. Natural Energy Decomposition Analysis of the Alkali Metal Complexes of 18c6[a]

	sym	ΔE	ES	CT	DEF (M^+)	DEF(18c6)	DIS(18c6)
Li^+	S_6	−89.1	−192.9	−91.1	7.4	146.2	41.3
	D_{3d}	−86.8	−122.4	−36.2	0.1	57.3	14.4
Na^+	C_1	−78.8	−171.9	−57.3	11.0	115.4	23.9
	D_{3d}	−81.7	−129.2	−33.5	2.3	66.1	12.7
K^+	D_{3d}	−68.1	−129.0	−27.1	16.7	62.4	8.9
Rb^+	C_{3v}	−55.2	−114.9	−24.9	18.1	57.8	8.7
	D_{3d}	−52.8	−129.5	−31.1	28.4	71.8	7.6
Cs^+	C_{3v}	−44.6	−99.8	−20.0	18.5	48.1	8.6
	D_{3d}	−30.4	−131.9	−34.0	46.9	79.9	8.7

[a] RHF/6-31+G* values. Energies in kcal mol^{-1}. *ES* = electrostatic interaction (eq 5). *CT* = charge transfer (eq 7). *DEF* = deformation (eq 4). *DIS* = geometric distortion (see text and eq 2).

CH bonds, 18.8−20.7%. This suggests the oxygen center polarizes the CH bond toward carbon to enhance the electrostatic interaction of each CH···O linkage. NBO analysis also reveals two delocalizing CH···O interactions of −0.6 kcal mol^{-1} each involving the oxygen hybrid lone pair and the CH antibonding orbital. Although rather weak, these intramolecular "charge transfer" interactions together account for 1.2 kcal mol^{-1} (or almost 25%) of the 4.4 kcal mol^{-1} energy difference separating the C_i and D_{3d} forms. Thus, it appears that electrostatic and delocalization effects in concert stabilize the C_i conformation.

Evidence of unfavorable O···O interactions appears in the analysis of the D_{3d} structure. The natural charges and CO bond ionicities reflect polarization of electron density away from the cavity toward the methylene groups. The average charge of an oxygen center is slightly more positive in the D_{3d} conformation than that of the C_i form (−0.694 vs −0.710), and the CO bonds are somewhat less polarized toward oxygen (C^+O^- bond ionicity is 37.7% compared to 38.4% for C_i). Such polarization likely arises from repulsive O···O interactions within the crown ether cavity.

Analysis of the M^+/18c6 complexes provides insight into the various factors that influence structure and cation binding strengths. We first examine the set of D_{3d} complexes which serves as a basis for comparison with the lower symmetry structures discussed below. The results in Table 4 reveal that electrostatic interaction is the dominant stabilizing component. ES is remarkably constant at roughly −129 kcal mol^{-1} over the range of metal cations, except for Li^+ (−122 kcal mol^{-1}).

(42) We report atomic populations to 0.001*e* as variations of this magnitude are significant. Reed *et al.* (ref 35b) discussed the relationship between energy and population demonstrating that the energy stabilization (ΔE, in au) associated with a change in population (Δq, in *e*) is given by $\Delta E \approx k\Delta q$ (k is a constant of order unity). A change in population of 0.001*e* therefore corresponds to $\Delta E = 0.001$ au or roughly 0.6 kcal mol^{-1}.

Table 5. Binding Energies for the K^+/18c6·mH_2O and Cs^+/18c6·mH_2O Complexes as a Function of Hydration Number m and the Reaction Energies ΔE_{rxn} for eq 10[a]

	$m=0$	$m=1$	$m=2$
K^+/18c6·mH_2O	−68.1	−76.1	−80.5
		(−8.0)	(−4.4)
Cs^+/18c6·mH_2O	−44.6	−52.4	−58.5
		(−7.8)	(−6.1)
ΔE_{rxn}[b]	8.4	8.6	6.9

[a] RHF/6-31+G* values in kcal mol^{-1}. Incremental binding energies, $\Delta E(m) - \Delta E(m-1)$, are given in parentheses. Counterpoise corrected binding energies are evaluated with respect to infinitely separated fragments (K^+, 18c6 in the C_i conformation, and m water molecules). [b] Counterpoise corrected binding energies for the $K^+(H_2O)_5$ and $Cs^+(H_2O)_5$ complexes are −73.5 and −58.4 kcal mol^{-1}, respectively, at the RHF/6-31+G* level.

CT stabilization is also important and exhibits little dependence on cation type, but it remains substantially (four to five times) weaker than ES. Yamabe and co-workers[16] examined these components in their CNDO/2 study of M^+/18c6 ($M^+ = Na^+$, K^+), concluding that CT was the dominant interaction in each complex, stronger than ES. However, the properties of their wave functions appear to differ significantly from those reported here. For example, the analysis of their K^+/18c6 complex revealed that the valence 4*s* and 4*p* orbitals of the metal were fairly strongly occupied (0.089*e* and about 0.229*e*, respectively) by charge transfer from the oxygen lone pairs of the crown ether. In contrast, NPA of our ab initio wave functions shows these orbitals to be only weakly occupied (0.046*e* and 0.001*e*, respectively), the 4*p* orbitals contributing negligibly to the interaction.

It appears that cation size (rather than an electrostatic or charge transfer effect) is largely responsible for the *variation* of the binding energies with cation type. The D_{3d} binding energies weaken with increasing size from −86.8 kcal mol^{-1} for Li^+ to −30.4 kcal mol^{-1} for Cs^+. DEF(M^+) and DEF(18c6) are the only energy components of Table 4 that show significant variation over the range of alkali metals. DEF(M^+) increases dramatically from 0.1 kcal mol^{-1} for Li^+ to 46.9 kcal mol^{-1} for Cs^+, while DEF(18c6) increases from 57.3 to 79.9 kcal mol^{-1}. Again, deformation is closely related to the Pauli repulsions experienced by the metal and crown ether fragments as their electronic distributions overlap. It is reasonable therefore that deformation of a large cation like Cs^+ in a relatively small cavity is greater than that of a smaller cation like Li^+ or Na^+. In contrast, the ES, CT, and DIS components reveal only marginal dependence on cation type.

NPA and NBO analysis (Table 3) on the D_{3d} structures reveal a weak but rather uniform polarization of the crown ether by the cation. The cation tends to draw a small amount of electron density from the methylenes toward the oxygen centers. Comparison of the average charge of a methylene group in the D_{3d} complex with that of the bare C_i 18c6 shows that 0.016*e* shifts from each methylene to its neighboring oxygen, regardless of cation type. Polarization of the crown ether is also seen in the percentage ionic character (C^+O^-) of the CO bond NBOs. The ionicity is remarkably constant (39.2−39.3%) over the full series of cation complexes and is somewhat greater than the average ionicity calculated for the uncomplexed C_i form (38.4%). Again this suggests that the metal cation draws electron density toward the cavity. Note that while these charges and population changes reflect important polarization effects, they are unable to provide any estimate of the strength of the polarization component of the cation/crown ether interaction.

The NEDA results of Table 4 also reveal why the cations other than K^+ favor 18c6 conformations other than D_{3d}. The ES and CT components are greatly enhanced in the lower symmetry conformations for Li^+ and Na^+. As discussed earlier, M^+···O distances are greatly reduced allowing for stronger Coulombic interactions and increased charge transfer from larger orbital overlap. At the same time, the DEF and DIS components become increasingly destabilizing but cannot overcome the favorable ES and CT interactions. In contrast, the relatively large Rb^+ and Cs^+ cations are displaced from the cavity. While this tends to weaken the ES and CT interactions, it more importantly reduces the Pauli repulsions (DEF components) that the cations experience in the cavity. Thus, Li^+ and Na^+ cations favor irregular conformations of 18c6 that reduce M^+···O distances and enhance ES and CT interactions, whereas Rb^+ and Cs^+ cations prefer to sit outside the crown ether cavity to avoid large Pauli repulsions.

Again, the charges and bond ionicities of Table 3 support the NEDA results. Comparison of the metal charges for the D_{3d} and low symmetry complexes reveals greater charge transfer in the latter. For example, the charge on the Li^+ center decreases from 0.939 in the D_{3d} complex to 0.901 for S_6, an increase of 0.038*e* transferred from 18c6 to the metal cation. Polarization of the crown ether is also greater in the low symmetry cases, leading to increased electrostatic interaction. The percentage ionic character increases somewhat (from 39.3% to 39.9% in the Li^+ complex), and the methylene group charges reflect greater polarization of the CO bonds toward the oxygen centers in the low symmetry complexes. The opposite trends are calculated for the Rb^+ and Cs^+ complexes. The charge of the metal center increases as the metal leaves the cavity (e.g., from 0.960 to 0.969 for Cs^+) suggesting somewhat weaker charge transfer interaction in the C_{3v} complexes, and the bond ionicity and methylene group charges show diminished polarization of the CO bonds (although they remain more polar than the CO bonds of the uncomplexed C_i structure).

V. Cation Selectivity

Binding selectivity is often associated with the ionic radius of the cation and the size of the crown ether cavity that it will occupy, the larger the mismatch, the less likely that the cation binds favorably.[4,7,43] The potassium selectivity of 18c6 lends support to this line of reasoning. The K^+ cation with ionic radius 1.38 Å is of perfect size to occupy the cavity of 18c6, having a radius of 1.34−1.43 Å.[44] All other alkali metal cations are either too small (Li^+ and Na^+ of radii 0.76 and 1.02 Å, respectively) or too large (Rb^+ and Cs^+ of radii 1.52 and 1.67 Å, respectively).[45] The binding energies of Table 2 reveal, however, that cation size alone cannot fully account for the observed selectivity. Indeed, while Li^+ and Na^+ are both too small to fill the cavity, they still bind more strongly to 18c6 than K^+ (by about 25 and 9 kcal mol^{-1}, respectively).

Solvation of the crown ether is known to strongly influence selectivity.[3,6,9,16] For instance, the observed selectivity sequence for dibenzo−18−crown−6 in polar solvents like water and methanol is $K^+ > Na^+ \sim Rb^+ > Cs^+$, whereas it is $Na^+ > K^+ > Rb^+ > Cs^+$ in apolar aprotic solvents such as acetonitrile.[3] That is, the binding preference for Na^+ or K^+ depends on solvent

(43) Hancock, ref 7, offers an alternative explanation of cation selectivity based on the size of the chelate rings formed by complexation of M^+ to the macrocycle.

(44) Dalley, N. K. In *Synthetic Multidentate Macrocyclic Compounds*; Izatt, R. M., Christensen, J. J., Eds.; Academic: New York, 1978; pp 207−243.

(45) Ionic radii taken from Shannon, R. D. *Acta Crystallogr.* **1976**, *A32*, 751.

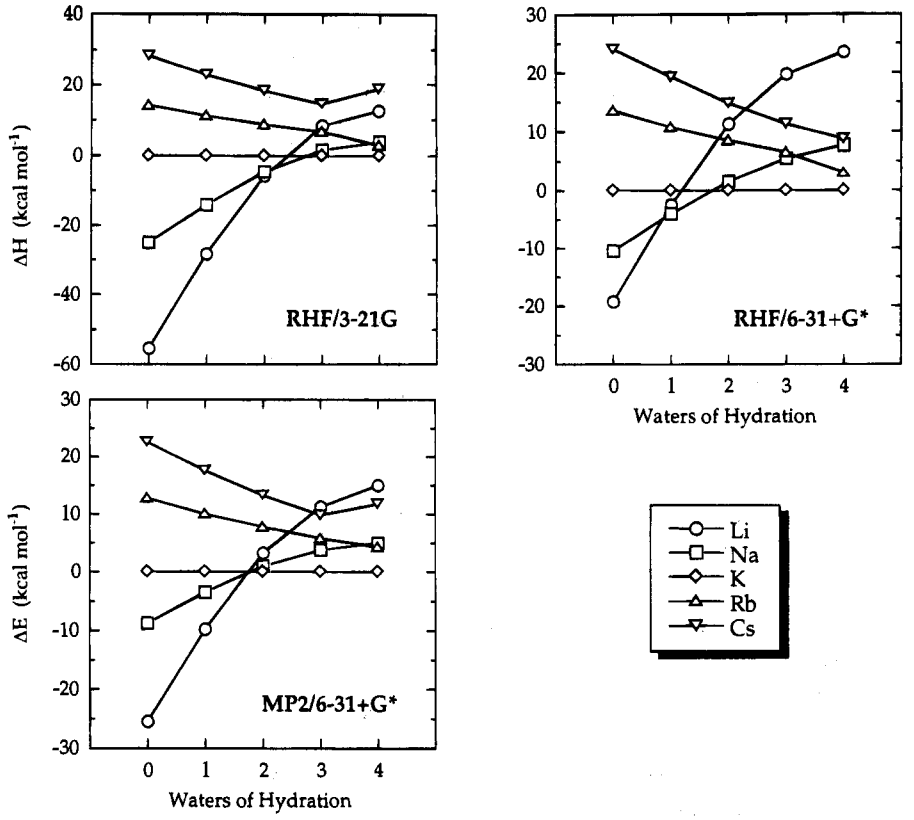

Figure 11. Reaction energies and enthalpies for the exchange reactions of eq 8 for the three levels of theory, RHF/3-21G, RHF/6-31+G*, and MP2/6-31+G*. The data points for the latter were calculated at the RHF/6-31+G* optimized crown ether complex and cluster geometries.

polarity. Selectivity is apparently the result of a delicate balance of the forces that the cation experiences as the crown ether and solvent molecules compete for the cation in solution. The binding energies that we report in Table 2, and the selectivity that one might judge from them, correspond to gas-phase quantities and are not, therefore, directly comparable to solution data. These data then suggest that the gas-phase sequence for 18c6 is $Li^+ > Na^+ > K^+ > Rb^+ > Cs^+$, quite distinct from the potassium selectivity observed in polar environments. Note that this sequence differs from that recently reported for the gas-phase by Maleknia and Brodbelt.[46] They applied the kinetic method in a collision-induced dissociation, liquid secondary ion mass spectrometry study of mixed crown ether/alkali halide complexes. Based on the abundance of product ions, they inferred a binding selectivity for 18c6 of $Na^+ \geq K^+ > Li^+ > Rb^+ > Cs^+$.

To investigate the role of aqueous solvent, we examine the exchange reaction

$$K^+/18c6 + M^+(H_2O)_n \rightarrow K^+(H_2O)_n + M^+/18c6 \quad (8)$$

in which a metal cation M^+, coordinated by $n = 0-4$ waters of hydration, displaces a K^+ cation from 18c6. The exothermicity (or exoergicity) of this reaction can be considered a measure of selectivity for the various cations ($M^+ = Li^+$, Na^+, K^+, Rb^+, and Cs^+). Wipff *et al.*[6] previously reported a selectivity of $Rb^+ > K^+ > Na^+$ for eq 8 and $n = 6$ using a molecular mechanics approach. We optimized each of the $M^+(H_2O)_n$ clusters at the RHF/3-21G and RHF/6-31+G* levels of theory and calculated MP2 correlation corrections at the 6-31+G* geometries. Although the larger ($n = 3$, 4) clusters have several stable structures, we only considered those of lowest energy, generally structures in which each water molecule directly coordinates the metal. The geometries, binding energies, and binding enthalpies of the $M^+(H_2O)_n$ clusters are described in detail elsewhere.[47] Figure 11 shows the reaction enthalpies (or energies for MP2) for eq 8 as a function of cluster size n for three levels of theory. The K^+ values (ΔH or $\Delta E = 0$) serve as a baseline, any point below this line suggesting the favorable displacement of K^+ from 18c6.

The cation selectivity for a particular cluster size n is determined by reading the data points of Figure 11 from bottom (corresponding to the most exothermic reaction) to top (the most endothermic). Thus, at each level of theory, we find that the gas-phase ($n = 0$) selectivity is $Li^+ > Na^+ > K^+ > Rb^+ > Cs^+$. The sequence changes, however, when one considers cation solvation. For $n = 4$, the three levels of theory give the following selectivities:

$$\text{RHF/3-21G: } K^+ > Rb^+ \sim Na^+ > Li^+ > Cs^+$$

$$\text{RHF/6-31+G*: } K^+ > Rb^+ > Na^+ \sim Cs^+ > Li^+$$

$$\text{MP2/6-31+G*: } K^+ > Rb^+ \sim Na^+ > Cs^+ > Li^+$$

In each case, 18c6 preferentially binds K^+ followed closely by Rb^+ and Na^+. The sequence is also somewhat dependent on level of theory. For example, RHF/3-21G suggests that 18c6 binds Li^+ more favorably than Cs^+, while RHF/6-31+G* shows the binding of Na^+ to be closer to Cs^+ than Rb^+.

For comparison, the experimentally determined selectivity for the fully solvated reaction

$$K^+/18c6(aq) + M^+(aq) \rightarrow K^+(aq) + M^+/18c6(aq) \quad (9)$$

is $K^+ > Rb^+ \sim Na^+ > Cs^+$. There are no experimental data for Li^+. Figure 12 shows the experimental reaction enthalpies

(46) Maleknia, S.; Brodbelt, J. *J. Am. Chem. Soc.* **1992**, *114*, 4295.

(47) Glendening, E. D.; Feller, D. (in preparation). Also see ref 31b.

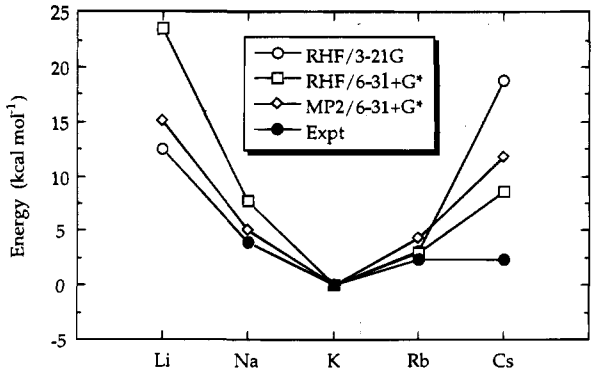

Figure 12. Comparison of the experimental determined reaction enthalpies for eq 9 with the $n = 4$ calculated values for eq 8. Enthalpy values are reported for RHF/3-21G and RHF/6-31+G*. Energy values are given for MP2/6-31+G*.

for eq 9 together with the $n = 4$ calculated values of eq 8.[48] The comparison is quite favorable for Na^+ and Rb^+. The calculated cluster reaction enthalpies differ from the experimental solution values by only a few kcal mol^{-1}. The comparison for cesium, on the other hand, is rather poor but not particularly surprising. The exchange reaction of eq 8 does not account for the full solvation of the cation or the solvation of the M^+/18c6 complexes.

The calculation of free energy changes for eq 8 would be particularly useful for comparison with experimental data that are often tabulated in terms of free energies (ΔG) or related association constants ($\log K$).[3,4,48] However, a reliable ab initio evaluation of these quantities is unlikely since the vibrational contributions to ΔS depend sensitively on low frequency modes. For instance, the $T\Delta S$ contribution ($T = 298$ K) to the binding free energy of $Cs^+(H_2O)_4$ changes considerably from -21.2 to -19.8 kcal mol^{-1} (a difference of 490 cm^{-1}) with only a 10 cm^{-1} variation in the frequency of the lowest vibrational mode. This suggests that the low frequency vibrations must be calculated to better than 10 cm^{-1} to obtain kcal mol^{-1} accuracy for the entropy. In contrast, ΔH is insensitive to variations of similar magnitude, remaining constant at -42.2 kcal mol^{-1} with a 10 cm^{-1} change in the highest vibrational mode (the mode that contributes most strongly to the vibrational enthalpy correction). The calculated frequencies are not accurate to even 10 cm^{-1}, and hence it appears that free energies cannot be reliably evaluated by ab initio methods.

We extended the Cs^+ exchange reaction of eq 8 to $n = 5$ and added waters of hydration to both the reactant K^+/18c6 and product Cs^+/18c6 complexes as follows:

$$K^+/18c6{\cdot}mH_2O + Cs^+(H_2O)_5 \rightarrow K^+(H_2O)_5 + Cs^+/18c6{\cdot}mH_2O \quad (10)$$

($m = 1,2$). These complexes and the $K^+(H_2O)_5$ and $Cs^+(H_2O)_5$ clusters were optimized at the RHF/6-31+G* level. Since the calculations of the M^+/18c6·mH_2O complexes are quite expensive, we discontinued geometry optimization when the total energy was converged to roughly 10^{-5} au (~0.01 kcal mol^{-1}). Our experience with the smaller complexes suggested that the binding energies were essentially converged at this point, while the geometrical features might vary somewhat if optimization were continued to full convergence of the gradients. The water molecules directly coordinate the metal of the crown ether complex in each case. In K^+/18c6·$2H_2O$, the cation sits near the center of the crown ether cavity, equatorially coordinated by the crown ether oxygens with a water molecule occupying each of the axial positions, one above and one below the crown ether. In Cs^+/18c6·$2H_2O$, the cation remains well outside the crown ether cavity (as seen for Cs^+/18c6) with both water molecules coordinating the metal from one side of the crown ether. The binding energies of the M^+/18c6·mH_2O complexes are listed in Table 5 together with the reaction energies for eq 10 as a function of hydration number m.

Solvating the M^+/18c6 complexes weakly influences the energetics of the exchange reaction, slightly favoring the formation of Cs^+/18c6. The exoergicity of eq 10 increases negligibly from 8.4 to 8.6 kcal mol^{-1} with addition of the first water of hydration. The second water has a somewhat larger effect, decreasing the exoergicity to 6.9 kcal mol^{-1}. The incremental binding energies reveal that the first water molecule stabilizes the two complexes by roughly equal amounts, 8.0 and 7.8 kcal mol^{-1} for K^+ and Cs^+, respectively, and, hence, has little influence on the exchange reaction. On the other hand, the incremental binding energies for the second water molecule differ somewhat, 4.4 and 6.1 kcal mol^{-1} for the K^+ and Cs^+ complexes, respectively. This difference reflects the more favorable interaction of water with the Cs^+ complex where the cation center is significantly displaced from the interacts more weakly with the crown ether cavity. We suspect that adding additional waters of hydration to these complexes will further stabilize (although slightly) Cs^+/18c6 in relation to the K^+ complex, but we anticipate that the selectivity sequences listed above would remain largely unchanged.

VI. Summary

We have presented a detailed ab initio study of the structure of 18-crown-6 (18c6) and its interaction with the alkali metal cations Li^+, Na^+, K^+, Rb^+, and Cs^+. A limited search for equilibrium geometries was performed for the uncomplexed 18c6 and for each of its cation complexes. In general, the calculated geometries compare quite favorably with published crystal structures. The methods employed suggest that the C_i conformation of 18c6 is 4–5 kcal mol^{-1} more stable than the D_{3d} form. The K^+ cation is of perfect size to occupy the crown ether cavity and therefore forms a complex of D_{3d} symmetry with the cation sitting at the center of the cavity. The Li^+ cation is too small to fully occupy the cavity so that the crown ether backbone tends to collapse around this cation in a conformation of lower (S_6) symmetry. The crown ether conformation favored by Na^+ was found to depend on the level of theory employed. At the RHF/3-21G level, the Na^+/18c6 complex favors a structure of C_1 symmetry, but higher level RHF and MP2 calculations with the 6-31+G* basis suggests that the D_{3d} form is preferred. The Rb^+ and Cs^+ cations are too large to fit into the cavity of 18c6 and hence reside outside in a structure of C_{3v} symmetry.

Our best estimates for the binding enthalpies of the K^+/18c6 and Cs^+/18c6 complexes are significantly stronger (by roughly 30 and 12 kcal mol^{-1}, respectively, at the MP2/6-31+G* level) than the experimentally determined values. Higher level calculations with more extended basis sets on the K^+/dimethyl ether prototype system suggest that the binding energies may be overestimated by as much as 5–7 kcal mol^{-1}. Clearly, this cannot fully account for the large discrepancy between the calculated and experimental values. This suggests that the experimental values of the M^+/18c6 binding enthalpies need to be redetermined.

Finally, solvation effects strongly influence the cation selectivity of the 18c6. Gas-phase 18c6 preferentially binds the small alkali metals cations relative to the larger ones. However, in

(48) Izatt, R. M.; Terry, R. E.; Haymore, B. L.; Hansen, L. D.; Dalley, N. K.; Avondet, A. G.; Christensen, J. J. *J. Am. Chem. Soc.* **1976**, *98*, 7620.

solution the crown ether and solvent molecules compete for the cations. We show that the selectivity sequence observed for 18c6 in aqueous environments is recovered when even a few water molecules are considered in a cation exchange reaction.

Acknowledgment. The authors would like to thank Dr. Thom H. Dunning, Jr., for his encouragement and contributions during the course of this investigation. This research was supported by the U.S. Department of Energy under Contract No. DE-AC06-76RLO 1830. The authors acknowledge the support of the Division of Chemical Sciences, Office of Basic Energy Sciences. E.D.G. also acknowledges the support of Associated Western Universities, Inc. (on behalf of Washington State University) under Grant No. DE-FG06-89ER-75522 with the U.S. Department of Energy. Portions of this work were completed on the computer resources at the National Energy Research Supercomputer Center with a grant provided by the Scientific Computing Staff, Office of Energy Research, U.S. Department of Energy. The Pacific Northwest Laboratory is a multiprogram national laboratory operated by Battelle Memorial Institute.